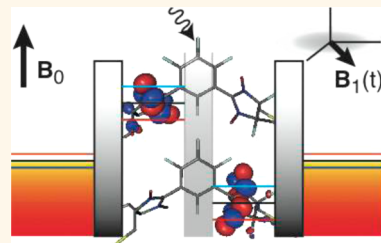


# Organic Single Molecular Structures for Light Induced Spin-Pump Devices

Burkhard O. Jahn,<sup>†</sup> Henrik Ottosson,<sup>†,\*</sup> Michael Galperin,<sup>‡</sup> and Jonas Fransson<sup>§,\*</sup>

<sup>†</sup>Department of Chemistry, BMC, Box 576, Uppsala University, 751 23 Uppsala, Sweden, <sup>‡</sup>Department of Chemistry and Biochemistry, University of California San Diego, La Jolla, California 92093, United States, and <sup>§</sup>Department of Physics and Astronomy, Uppsala University, Box 530, SE-751 21 Uppsala, Sweden

**ABSTRACT** We present theoretical results on molecular structures for realistic spin-pump applications. Taking advantage of the electron spin resonance concept, we find that interesting candidates constitute triplet biradicals with two strongly spatially and energetically separated singly occupied molecular orbitals (SOMOs). Building on earlier reported stable biradicals, particularly *bis*(nitronyl nitroxide) based biradicals, we employ density functional theory to design a selection of potential molecular spin-pumps which should be persistent at ambient conditions. We estimate that our proposed molecular structures will operate as spin-pumps using harmonic magnetic fields in the MHz regime and optical fields in the infrared to visible light regime.



**KEYWORDS:** biradicals · single molecule · spin current · spin-pump · spintronics · triplet state

Questions of spin-charge separation and control of spin in quantum devices are under general focus and activity within the physical, chemical, and engineering sciences. Since the conceptual introduction of spintronics and magnetoelectronics,<sup>1,2</sup> a critical issue to be resolved is the generation of pure spin currents, for which magnetic metallic layered set-ups have been proposed.<sup>3</sup> Experimentally, the generation of spin current has been observed in layered spin-pump devices<sup>4</sup> and also in quantum dots.<sup>5</sup> In parallel with that of the solid state branch, there is great activity in the fields of organic<sup>6</sup> and molecular spintronics<sup>7</sup> and approaching the single molecular limit for inorganic single molecule magnets,<sup>8</sup> as well as proposals for molecular logic gates.<sup>9</sup>

Traditionally, spin flux is considered to be controlled by a magnetic field while recent studies indicate additional control of spin using electric potential and optical excitations. Theoretical studies of an electron spin resonance (ESR) setup for molecular systems demonstrate the possibility of the construction of a molecular spin-pump which leads each electronic spin projection ( $\alpha \uparrow, \beta \downarrow$ ) in different spatial directions, while the net charge current is negligible.<sup>10</sup>

Herein, we propose organic molecular systems that would be suitable for experimental realization of the spin-pump device.<sup>11</sup>

As will be briefly discussed below, interesting molecules are biradicals, which in their electronic ground state assume a triplet multiplicity configuration and which have two singly occupied molecular orbitals (SOMOs) that are strongly spatially and energetically separated. These requirements can be fulfilled by the linkage of two radical units (RUs) *via* a bridging unit (BU) which could be saturated or  $\pi$ -conjugated, where the  $\pi$ -conjugated BU must be connected so that it functions as a ferromagnetic coupling unit giving the high-spin triplet biradical as the ground state.<sup>12</sup> Several stable radical and biradical building blocks are known, and the mounting of radical species onto surfaces has also been considered.<sup>13,14</sup> Potential templates which agree with the theoretical model and the stability requirements are the *bis*(nitronyl nitroxide) based biradicals developed by Matsuda and co-workers.<sup>15</sup> These contain linking groups that can be tuned by derivatization and also an insulating saturated BU in the middle.

The stable triplet carbene molecules of the Tomioka group<sup>16</sup> ensured by a cumulated allenic system are interesting; however, they do not show the same long-term persistence. To ensure the triplet biradical ground state, two nitronyl nitroxide radicals can be coupled through a *meta*-substituted benzene ring, which leads to a persistent triplet biradical as shown by Takui.<sup>17</sup> Finally, the

\* Address correspondence to  
henrik.ottosson@kemi.uu.se,  
jonas.fransson@physics.uu.se.

Received for review August 23, 2012  
and accepted January 15, 2013.

Published online January 25, 2013  
10.1021/nn3038622

© 2013 American Chemical Society

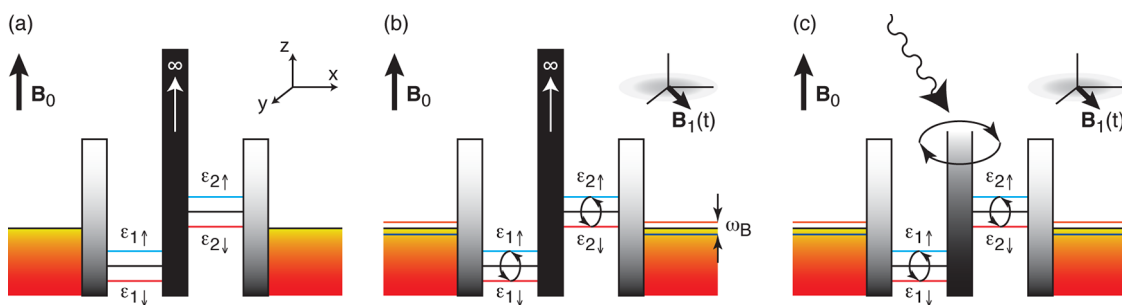


**Figure 1.** Schematic illustration of the spin-pump. (a) Two uncoupled orbitals which are connected to external electrodes and Zeeman split by the constant external magnetic field  $B_0$ . (b) A harmonic external magnetic field  $B_1(t)$  provides a coupling between the spin projections of each orbital and a spin bias in the external electrodes. (c) An irradiation field generates a finite coupling between the molecular orbitals.

recent aza-*m*-xylylene based triplet biradicals of Rajca and co-workers<sup>18</sup> are also interesting.

On the basis of these previous fundamental studies we designed candidates for realistic molecular spin-pumps and studied these by computational means. The envisioned single molecular spin-pump devices could potentially be generated using the mechanically controlled break-junction technique, by which charge transport through single molecules is regularly studied.<sup>19</sup> Such a setup requires additional anchor groups and our molecules therefore have thiol end groups. Thus, the goal of the present study has been to test the theoretical foundations for single molecule spin-pumps on molecular structures which potentially could be the ones that will be examined experimentally.

## RESULTS AND DISCUSSION

First, we briefly introduce the theoretical model that provides the foundation for finding suitable molecular structures. The second part of the study is devoted to the design of suitable molecular candidates, and also to the identification of problematic features that an efficient single molecular spin-pump (SMSP) should not display.

**Theory and Modeling.** Initially, the SMSP should constitute two spin-degenerate orbitals, at the energies  $\varepsilon_i$ ,  $i = 1, 2$ , which are separated both in space and energy, so that there is only a negligible overlap between them (see Figure 1a). Each end of the SMSP is connected to an electrode, and we describe the coupling using the Hamiltonian

$$\mathcal{H}_T = \sum_{\mathbf{p} \in L} v_{\mathbf{p}1} c_{\mathbf{p}\sigma}^\dagger d_{1\sigma} + \sum_{\mathbf{q} \in R} v_{\mathbf{q}2} c_{\mathbf{q}\sigma}^\dagger d_{2\sigma} + H.c.$$

where  $c_{\mathbf{k}\sigma}^\dagger$ ,  $\mathbf{k} = \mathbf{p}, \mathbf{q}$ , creates an electron in the electrode  $\chi = L, R$ .<sup>10,20</sup> The operator  $d_{i\sigma}$  destroys an electron of spin  $\sigma = \uparrow, \downarrow$ , in orbital  $i$  in the SMSP, whereas  $v_{\mathbf{k}i}$  is the tunneling rate. Application of a static magnetic field  $\mathbf{B}_0 = B_0 \hat{\mathbf{z}}$  provides a Zeeman split of the orbital energies, that is,  $\varepsilon_i \rightarrow \varepsilon_{i\sigma} = \varepsilon_i - \sigma^z g \mu_B B_0 / 2$  ( $\sigma^z$  is the  $z$  Pauli matrix), and we define the Larmor frequency  $\omega_L = |\varepsilon_{i\uparrow} - \varepsilon_{i\downarrow}| = g \mu_B B_0$ , while the electrodes are assumed to have a negligible susceptance to external magnetic fields (see Figure 1a for coordinates).

Next, we apply a harmonic magnetic field  $\mathbf{B}_1(t) = B_1(\hat{\mathbf{x}} \cos \omega_B t + \hat{\mathbf{y}} \sin \omega_B t)$ , which creates

a coupling between the spin states  $\varepsilon_{i\sigma}$  through

$$\mathcal{H}_{sf} = -g \mu_B B_1 \sum_i d_{i\uparrow}^\dagger d_{i\downarrow} e^{i\omega_B t} + H.c.$$

The coupling introduced between the spin states in the molecule along with their tunneling coupling to the electrodes, generates a spin bias  $\mu_\uparrow - \mu_\downarrow = \omega_B$  in the electrodes (see Figure 1b) where  $\mu_\sigma = \mu + \sigma^z \omega_B / 2$  is the spin-chemical potential in the electrode defined with respect to the electrochemical potential  $\mu$ .<sup>21,22</sup> By variation of the magnetic field frequency  $\omega_B$ , the system can be tuned into a resonant regime (ESR) in which a non-negligible spin current flows between the spin-chemical potentials in the electrode *via* spin-flip processes in the molecular orbitals.

As the molecular orbitals  $\varepsilon_i$ ,  $i = 1, 2$ , are initially uncoupled, we introduce a controlled entanglement between them by application of the field<sup>10,20</sup>

$$\mathcal{H}_V = 2\mathcal{R}(V_E e^{-i\omega_E t}) \sum_\sigma d_{1\sigma}^\dagger d_{2\sigma} + H.c.$$

with strength  $V_E$  and frequency  $\omega_E$ . The coupling field may originate from, for example, light irradiation in the infrared to visible regime, and will henceforth be referred to as the irradiation field (see Figure 1c).

Following the procedure in ref 20, we transform the system into the rotating reference frame and employ the rotating wave approximation. This results in an effective steady-state problem (see refs 10 and 20 for details). The result of this transform is that the local density of electron states (DOS) around orbital  $i$  can be viewed as a series of peaks in addition to the central peak located near the bare level  $\varepsilon_i$  (see eq 3 in what follows and Figure 2a). Because of the induced coupling between the orbitals, electrons can flow between the left and right electrodes, given that a bias voltage is applied across the molecular junction. As we herein focus on the regime where the resonant frequency  $\omega_r$  is much larger than the strength of the transverse magnetic field; that is,  $(2g\mu_B B_1/\omega_r)^2 \ll 1$ , and since we wish to provide a qualitative picture of the processes involved, we find that the spin projected currents between the left electrode and the molecule can

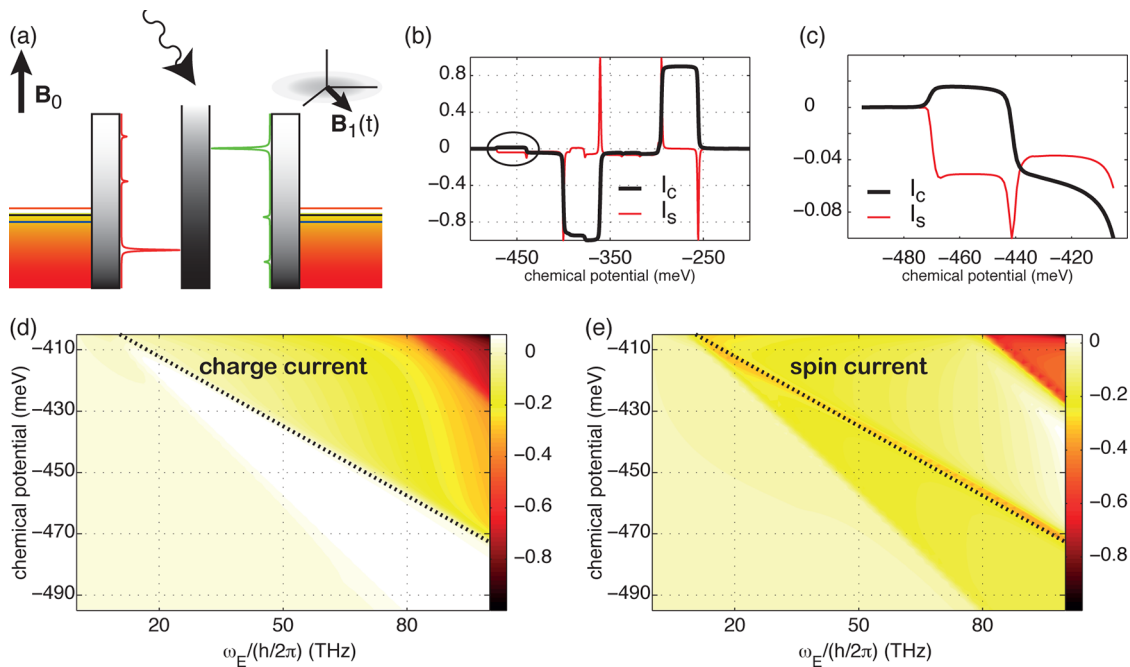


**Figure 2.** (a) Schematic illustration of the local DOS for the orbitals 1,2 in the presence of the harmonic magnetic field and irradiation field. (b) Charge current ( $I_c$ , bold) and spin current ( $I_s$ , faint) as a function of the electrochemical potential  $\mu$ , given  $\omega_E\hbar = 60$  THz. (c) Close up of the charge and spin currents in the encircled regime in panel b. (d,e) Contour plots of (d) the charge current and (e) the spin current as function of the frequency  $\omega_E$  and electrochemical potential. For the plots in panels b and c we have used  $\varepsilon_1 = -390$  meV,  $\varepsilon_2 = -305$  meV,  $\omega_B\hbar = 500$  MHz,  $B_0 = 1$  T,  $B_1 = 0.01$  T,  $V_E = 20$  meV,  $\Gamma_i = 0.5$  meV, and  $V = 0$  mV.

be approximated by

$$I_{R\sigma} = \frac{e}{\hbar} |V_E|^2 \Gamma_1 \Gamma_2 \sum_{n=\pm 1} \int \frac{f_{L\sigma}(\omega) - f_{R\sigma}(\omega + n\omega_E)}{(\omega + n\omega_E - \varepsilon_{2\sigma})^2 + \Gamma_2^2/4} |G_{1\sigma}^r(\omega)|^2 d\omega \quad (1)$$

An analogous expression can be derived for the current  $I_{R\sigma}$  for the current between the right electrode and orbital 2. Here,  $G_{1\sigma}^r$  is the dressed retarded Green function (GF) for the orbitals 1 in the presence of the irradiation field applied to the molecule. The Lorentzian  $[(\omega + n\omega_E - \varepsilon_{2\sigma})^2 + \Gamma_2^2/4]^{-1}$  appearing in the expression for the current is a result of the coupling between the orbitals 1 and 2 and reflects the fact that the electrons tunneling to (from) the left electrode may originate from (terminate at) orbital 2. The physical mechanism behind this is discussed further below. The parameters  $\Gamma_i$ ,  $i = 1, 2$ , define the couplings between the left (right) electrode and orbital 1 (2), whereas  $f_{\chi\sigma}(\omega) = f(\omega - \mu_{\chi\sigma})$  denotes the Fermi function for the spin channel  $\sigma$  in electrode  $\chi$ .

The form of the current in eq 1 can be understood from the following discussion. In the limit  $(2g\mu_B B_1/\omega_r^2 \ll 1)$ , the bare GF  $G_{2\sigma}^{(0),r}$  for orbital 2 is approximately given by

$$G_{2\sigma}^{(0),r}(\omega) = \frac{1}{\omega - \varepsilon_{2\sigma} + i\Gamma_2/2} \quad (2)$$

suggesting that the spin channels can be regarded as independent of one another. Similarly, within the given limit the dressed GF  $G_{1\sigma}^r$  for orbital 1 is also approximately independent of the opposite spin channel; however, it is

influenced by the coupling to orbital 2. We can write the GF as

$$G_{1\sigma}^r(\omega) = \frac{1}{\omega - \varepsilon_{1\sigma} - |V_E|^2 \sum_{n=\pm 1} G_{2\sigma}^{(0),r}(\omega + n\omega_E) + i\Gamma_1/2} \quad (3)$$

While this expression clearly suggests that there is a main peak centered near  $\varepsilon_{1\sigma}$ , it moreover indicates the existence of additional peaks located near  $\varepsilon_{2\sigma} \pm \omega_E$ . In Figure 2 we plot the typical local DOS ( $-\mathcal{J} \sum_{\sigma} G_{1\sigma}^r / \pi$ ) for the molecular orbitals, which readily indicates the side peaks in the vicinity of the main peak of the adjacent orbital.

The induced electronic structure enables electron transport between electrodes. However, the system has to be gated such that the molecular orbitals are positioned on either side of the Fermi level as is indicated by panel (b) in Figure 2, where the charge (bold) and spin (faint) currents are shown as function of the electrochemical potential  $\mu$ . The charge current is defined as the sum of the spin projected currents,  $I_c = \sum_{\sigma} (I_{L\sigma} - I_{R\sigma})/2$ , and we have defined current flowing from the left to the right electrode as positive (in the regime under consideration, the spin-nonconserving currents are negligible). Clearly, the charge current (amplitude) peaks at the positions of the molecular orbitals. Variations in the spin current, the spin current is defined by  $I_s = \sum_{\sigma} \sigma_{\sigma\sigma}^z (I_{L\sigma} - I_{R\sigma})/2$ , occur simultaneously with the changes in the charge current under the condition that the spin projected currents are nondegenerate (degenerate spin projected currents

implies a vanishing spin current). The plot in Figure 2b indicates that the spin current is strong in the present system nearby the molecular orbitals. It is clear from the plot that, for instance, the spin current can be forced to flow in the same or in the opposite direction as the charge current depending on the gating of the system. Such a feature may be used for spin-transistor applications since the sign of the spin current can be manipulated and controlled by variations in the overall electrochemical potential, or gate voltage (see Supporting Information).

Special attention is drawn, however, to the characteristics displayed in Figure 2c, corresponding to the encircled regime in Figure 2b. Here, the charge current changes sign (around  $-440$  meV) while simultaneously the spin projected currents are nonvanishing but with opposite signs, resulting in a nonvanishing spin current. Thus, the spin projected currents flow in opposite direction between the electrodes, something that might be used to accumulate spins of different projection at different ends of the system.

Gating the system to the regime where the charge current is close to zero, we sweep the frequency of the irradiation field and calculate the resulting charge and spin currents, shown in Figure 2 panels d and e, respectively. Those contour plots clearly illustrate that the charge current can be made arbitrarily small by tuning the frequency  $\omega_E$  of the irradiation field (bright region in panel d), while the spin current remains finite. The spin current  $I_s$  is roughly constant in the frequency range where the charge current vanishes.

**Molecular Design.** Next, we discuss our results considering a limited selection of molecular structures that may enable the realization of our proposed setup. Three differently substituted nitronyl nitroxide radicals (**1–3**) were employed as monoradical units. Two such monoradicals were linked by a few different types of bridging and linker units into SMSP candidates **4–9**. Additionally, SMSP candidate **10**, related to a recent stable triplet biradical of Rajca, was also studied computationally. Among these, SMSP candidate **9** is the most promising one (*vide infra*). Yet, rather than discussing merely the most promising SMSP candidates it should be instructive for the future molecular design of organic spin-pump molecules to progress the discussion in a stepwise manner and to present also the pitfalls in the design process. Our structures **1–10** were examined by quantum chemical calculations at (U)M06-2X hybrid meta density functional theory level<sup>23</sup> using the 6-311G+(d,p) valence triple- $\zeta$  basis set.<sup>24–26</sup> Analogous results from calculations using the (U)B3LYP hybrid functional<sup>27,28</sup> are given in the Supporting Information.

As we pointed out in the previous sections, the nitronyl nitroxide radical is stable at ambient conditions,<sup>29</sup> and therefore suitable as a RU in our SMSPs. To tune the energy level of the SOMO

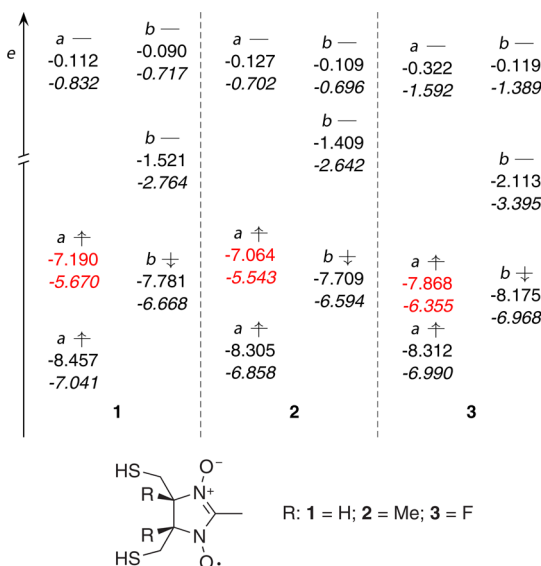


**Figure 3. Orbital energies  $\varepsilon$  (eV) of the monoradicals **1–3** at UM06-2X/6-311+G(d,p) and UB3LYP/6-311+G(d,p) (given in italics).  $\alpha$ -SOMO energies given in red ( $\varepsilon_1 = \varepsilon_{\text{SOMO}}$ ) and orbital numbers given in parentheses.**

( $\varepsilon_{\text{SOMO}}$ ) several substitution patterns were calculated as shown in Figure 3. In addition to the unsubstituted case, methyl and fluoro substituents were chosen to shift  $\varepsilon_{\text{SOMO}}$  up and down, respectively. For the unsubstituted nitronyl nitroxide **1** the  $\varepsilon_{\text{SOMO}}$  is  $-7.190$  eV at UM06-2X/6-311+G(d,p) level, while for **2** and **3**  $\varepsilon_{\text{SOMO}}$  is found at  $-7.064$  and  $-7.868$  eV. Thus, the variation of  $\varepsilon_{\text{SOMO}}$  between these three substitution patterns of the nitronyl nitroxide radical amounts to  $\sim 0.8$  eV. In contrast to the SOMOs, the energy levels of the neighboring MOs are much less affected by the change in substitution. For the  $\alpha$ -spin orbitals, radicals **1** and **2** have energy differences between the SOMO and the highest doubly occupied MO (HOMO) of more than  $1.2$  eV, while for the fluoro substituted **3** this  $\alpha$ -spin orbital separation is less than  $0.5$  eV. The SOMO is a  $\pi$ -type orbital localized over the  $N$ -oxide moieties while the HOMO is represented by the  $\pi$ -type lone-pairs at the sulfur atoms of the thiol groups which function as anchors of the single molecule spin-pump to gold electrodes. In the case of **2**, both SOMO and HOMO are delocalized to a larger extent and are not spatially separated.

Our SMSP candidates all consist of two RUs, a bridging unit, and thiol anchor groups (Figure 4). It can first be noted that five of the seven species are triplet biradicals in their electronic ground state and the open-shell singlet biradical state is higher in energy by  $14$ – $477$  meV ( $1.3$ – $46.0$  kJ/mol) according to calculations at UM06-2X/6-311+G(d,p) (see Supporting Information) with the smallest energy difference found for **7** and the largest for **10**. For two species, **4** and **5**, the open-shell singlet and the triplet states are essentially degenerate (with UM06-2X the singlet biradical is  $0.3$ – $0.5$  kJ/mol below the triplet).

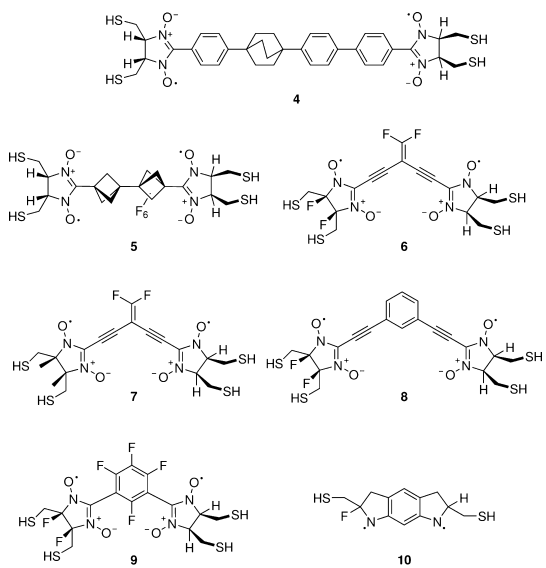


Figure 4. Structures of the SMSP candidates.

Two approaches are possible to design molecules with energetically and spatially separated SOMOs. First, the RUs can be different at the left and the right side (e.g., **1**, **2**, or **3**). Indeed, a range of different RUs could potentially be used, and the results reported here are therefore primarily a proof-of-principle study of a small selection of SMSP candidates that can be realizable. The second approach is to introduce additional linker units (LUs) between each RU and the central bridging unit, and by which the energy difference between the SOMOs at the two RUs,  $\Delta\varepsilon_{\text{SOMOs}} = |\varepsilon_1 - \varepsilon_2|$ , can be tuned. In this case the radical units do not necessarily need to be functionally different, and it is then sufficient to substitute one of the linker units or to introduce two different LUs. However, the usage of linker units which are chemically related but with different electron demands so as to create energetically separated SOMOs gives much smaller orbital splittings when compared to substitution directly at a radical unit. Yet, linking groups give a spatial expansion of the radical end-units of the spin-pump candidates, and this may be beneficial. The specific linking groups used herein are limited to phenyl and ethynyl groups. A summary of the orbital energies for compounds **4–9** is provided in Table 1. Two types of BUs were examined: (i) saturated (insulating) BUs such as different kinds of bicyclic groups, and (ii) BUs which provide for ferromagnetic coupling by inhibiting the combination of the two radicals to a closed-shell species, and thus, ensuring a high-spin configuration by spin polarization.<sup>30</sup> For example, the *m*-phenylene BU in combination with two methylene groups leads to *m*-xylylene, that is, a species with a triplet multiplicity ground state.<sup>31</sup> Similarly, the cross-conjugatively attached ethenyl BU forms a basis for the trimethylenemethane (TMM) triplet biradical.<sup>32</sup> For these latter two species the triplet state is more stable than the singlet state by

**TABLE 1. Orbital Energies of the Triplet States at UM06-2X/6-311+G(d,p) (Energy Units: eV)**

compound	spin	$\varepsilon_{\text{HOMO}}$	$\varepsilon_{\text{SOMO1}}$	$\varepsilon_{\text{SOMO2}}$	$\Delta\varepsilon_{\text{SOMOs}}$
<b>4</b>	$\alpha$	-7.674	-7.269	-7.240	0.029
	$\beta$	-7.173	-1.551	-1.523	
<b>5</b>	$\alpha$	-8.534	-7.525	-7.325	0.200
	$\beta$	-7.898	-1.767	-1.638	
<b>6</b>	$\alpha$	-8.334	-8.002	-7.471	0.531
	$\beta$	-7.659	-2.061	-1.679	
<b>7</b>	$\alpha$	-8.330	-7.390	-7.305	0.085
	$\beta$	-7.484	-1.544	-1.503	
<b>8</b>	$\alpha$	-8.313	-7.933	-7.388	0.545
	$\beta$	-7.520	-2.005	-1.659	
<b>9</b>	$\alpha$	-8.408	-8.082	-7.556	0.526
	$\beta$	-8.253	-2.250	-1.811	
<b>10</b>	$\alpha$	-8.173	-8.026	-7.574	0.452
	$\beta$	-8.071	-2.941	-2.672	

40.2 and 67.4 kJ/mol (417 and 699 meV), respectively, when based on negative ion photoelectron spectroscopy.<sup>33,34</sup> At the M06-2X/6-311+G(d,p) level the singlet-triplet energy gaps are calculated to be 46.5 and 95.8 kJ/mol, respectively. This relationship between the energies of the lowest singlet and triplet states is in agreement with the theory of disjoint and nondisjoint biradicals of Borden and Davidson which predicts that odd alternate hydrocarbons which are nondisjoint biradicals (e.g., TMM and *meta*-xylylene) have triplet multiplicity ground states.<sup>35</sup>

SMSP candidate **4** is based on earlier reported *bis*(nitronyl nitroxide) biradicals which could be synthesized and handled by standard organic synthesis techniques at ambient and slightly elevated temperatures.<sup>15</sup> This biradical type consists of two RUs **1** linked by a rod of *p*-phenylene groups. A bicyclo-[2.2.2]octyl segment in the midst of the *p*-phenylene rod serves as the BU. The only change in molecular design as compared to the earlier reported compound of Matsuda<sup>15</sup> is the replacement of two methyl groups at each RU to two methylthio groups to the RUs. The inequality between the two radical moieties of **4** is ensured by the different numbers of linking *p*-phenylene units (see Figure 4). However, since candidate **4** is best described as a pair of noninteracting monoradicals, this compound has a  $\Delta\epsilon_{\text{SOMOs}}$  of merely 29 meV and an essential degeneracy of the open-shell singlet and triplet states (the singlet biradical is below the triplet by 0.3 kJ/mol with UM06-2X). Moreover, it has an undesirable orbital pattern at the UM06-2X level because the highest occupied  $\beta$ -spin orbital is higher in energy than the two localized  $\alpha$ -spin SOMOs, and at UB3LYP level this  $\beta$ -spin orbital is further delocalized over the biphenyl segment. The shapes of the MOs are primarily the same, but at this level there are no interfering  $\beta$ -spin orbitals. By ensuring that there are no intruding  $\beta$ -spin orbitals at the UM06-2X level we find that there are also no such orbitals. SMSP candidate **5** is again a combination of two RUs **1** with a

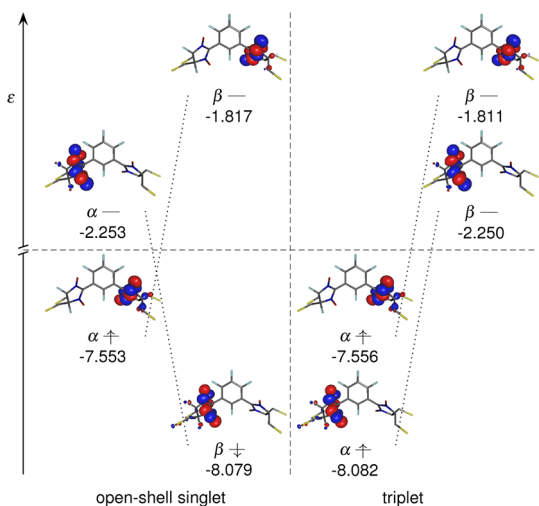


**Figure 5.** Highest occupied and lowest unoccupied molecular and spin orbitals for the singlet and triplet biradical states of compound **9**, calculated using UM06-2X/6-311+G(d,p). Dotted lines connect equivalent  $\alpha$  and  $\beta$  spin orbitals. Hydrogen atoms are omitted for clarity. (Energy units: eV).

saturated bicyclic coupling unit; however, in this case the BU is based on two bicyclo[1.1.1]pentyl units. This molecule is an example on how to create an energy splitting of the two SOMOs by fluoro substitution at one of the bicyclo[1.1.1]pentyl units. With 200 meV the  $\Delta\epsilon_{\text{SOMOs}}$  is larger than that of **4**, and the orbital window contains no intruding  $\beta$ -spin orbitals at the UM06-2X level, but the open-shell singlet and the triplet states are still degenerate. We can thus conclude that (i) with possibilities for spin delocalization away from the nitronyl nitroxide radical onto  $\pi$ -conjugated segments there is a risk that  $\beta$ -spin orbitals emerge within the  $\alpha$ -spin orbital window, and (ii) with saturated BUs it is not possible to clearly achieve a triplet multiplicity ground state. A BU which allows for ferromagnetic coupling is required.

The spin-pump candidate **6** consists of the RUs **1** and **3** in combination with two ethynyl LUs which are cross-conjugatively attached to a 2,2-difluoroethyl group, a ferromagnetic BU.<sup>36</sup> The relative energies of the two  $\alpha$ -SOMOs of **1** and **3** persist in **6** (see Figure 3), so that  $\Delta\epsilon_{\text{SOMOs}}$  amounts to 531 meV. However, molecule **6** shows the effect of an intruding  $\beta$ -spin orbital in between the two  $\alpha$ -SOMOs. This intruding  $\beta$ -spin orbital has  $\pi$ -type character and is delocalized over the ethynyl LUs and the BU (see Supporting Information). The introduction of RU **2** instead of **3** leads to spin-pump candidate **7**, for which the  $\Delta\epsilon_{\text{SOMOs}}$  amounts to only 85 meV, but due to the RU **2** the SOMO1 of **7** is higher in energy than in **6**, and this avoids the intruding  $\beta$ -spin orbital.

SMSP candidate **8** resembles **6**, with the difference being the *meta*-substituted phenyl moiety as a ferromagnetic BU. Consequently, with 546 meV the  $\Delta\epsilon_{\text{SOMOs}}$  of **8** is nearly the same as in **6**, and also **8** has an

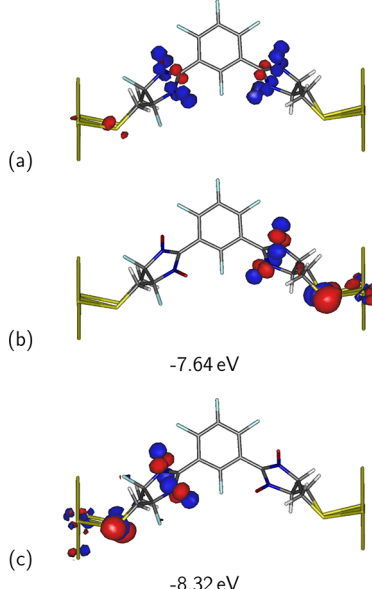


**Figure 6.** Spin-pump candidate **9** in its triplet state inserted between two small Au<sub>5</sub> clusters and the calculated (a) spin density (isovalue 0.02), (b) the highest alpha spin-orbital (SOMO2), and (c) next-highest alpha spin-orbital (SOMO1). Calculations performed at the M06-2X/LANL2DZ level.

intruding  $\beta$ -spin orbital which is energetically higher than SOMO1. Molecule **9** is again a combination of the RUs **1** and **3**, but without any linking units. It also has a perfluorinated *m*-phenylene as BU, which energetically pushes down the intruding  $\beta$ -spin orbital observed in **8**. With 526 meV the  $\Delta\epsilon_{\text{SOMOs}}$  of **9** is, as can be expected, in the similar range as that for molecules **6** and **8** which contain the same RUs. However, the intruding  $\beta$ -spin orbital is now removed (Figure 5).

In our set of SMSP candidates we also included molecule **10** derived from the aza-*m*-xylylene based biradicals of Rajca *et al.*<sup>18</sup> This candidate is related to molecule **9** as both have the RUs situated in *meta*-positions of bridging phenyl groups providing ferromagnetic coupling. Compared to the synthesized compound, **10** is a stripped version in which sterically congestive (and protective) groups have been omitted for computational reasons. We have also added thiol anchor groups, as well as a fluoro substituent at the saturated carbon adjacent to the nitrogen atom to ensure a large  $\Delta\epsilon_{\text{SOMOs}}$ . This substitution pattern leads to a  $\Delta\epsilon_{\text{SOMOs}}$  of 452 meV without any intruding occupied  $\beta$ -spin orbitals. However, the RUs and the small dimension of **10** lead to two SOMOs that both are delocalized over nearly the complete molecule, in disagreement with the requirement of two spatially separate SOMOs.

Thus, **9** is the most suitable compound to function as a SMSP among the candidates considered herein. This candidate is also closely related to a biradical which is persistent at ambient conditions.<sup>17</sup> Still, attachment in between the two Au electrodes may severely distort the molecular electronic structure from

what is desirable for the spin-pump application, for example, through electron donation from the metal to the molecule. Indeed, recent DFT studies of nitroxyl nitroxide radicals connected to thiol groups *via* phenyl and methyl phenyl groups displayed unexpectedly large coupling with Au.<sup>37</sup> We therefore examined **9** anchored on each side to two Au clusters, and performed computations at the M06-2X/LANL2DZ level.<sup>38,39</sup> These computations were complicated by very high amounts of spin-contamination for clusters with nine or more Au atoms (also when functionals without exact exchange, such as M06-L, were applied). We analyzed SMSP candidate **9** in its triplet state coordinated to two clusters with five Au atoms each, despite a rather spin contaminated Kohn–Sham solution ( $\hat{S}^2 = 3.46$ ). Yet, one can observe that the two SOMOs are located at each of the two separate RUs, and this is also where the spin density is predominantly located (Figure 6). Moreover, we do not find any donation of electrons from the metal clusters to the molecule. Thus, the limited data obtained from the calculation with the small clusters indicate that SMSP candidate **9** indeed retains its neutral triplet state biradical character when incorporated into a nanoelectrode setup, and it

should be an interesting target for synthesis and further experiments.

## CONCLUSIONS

We make theoretical predictions of molecular structures for realistic single molecule spin-pump applications. A selection of candidates were examined, and we find that compounds **7** and **9** meet the requirements of having triplet multiplicity ground states with spatially and energetically separated singly occupied molecular orbitals. These compounds are also beneficial from an applications point of view as they are closely related to previously reported triplet biradicals which are stable at ambient conditions. We estimate that our proposed structures will operate as spin-pumps for harmonic magnetic fields in the MHz regime and optical fields in the infrared to visible light regime. It should be noticed that not only time-varying magnetic fields may be employed to generate a spin-flip scattering between the molecular spin states, but other sources for spin-flip scattering may be provided by, e.g., circularly polarized light. Such a setup would open possibilities to create larger spin biases in the electrodes and would, thus, open access to a wider range of spin-current generations.

## COMPUTATIONAL METHODS

All DFT calculations were performed with the Gaussian 09 program package.<sup>40</sup> All geometries were optimized at the (U)M06-2X/6-311+G(d,p) hybrid meta DFT level of theory,<sup>23–26</sup> and at the (U)B3LYP/6-311+G(d,p) hybrid DFT level.<sup>27,28</sup> Open-shell singlet states were calculated by using the broken-symmetry formalism. In the case of B3LYP/6-311+G(d,p) some of the structures converged only to the closed-shell solution.

The computed values for the energy gaps between the triplet and open-shell singlet states ( $\Delta E_{ST}$ ) were corrected for spin contamination by usage of eq 4, where  $\Delta E_U$  is the energy gap obtained through the unrestricted solution for the singlet state and the  $\hat{S}_{T/S}^2$  are the computed values of the  $\hat{S}^2$  operator revealing the degree of spin contamination.

$$\Delta E_{ST} = \Delta E_U \frac{\hat{S}_T^2}{\hat{S}_T^2 - \hat{S}_S^2} \quad (4)$$

We also calculated the  $\Delta E_{ST}$  when regarding the closed-shell singlet state by usage of the restricted solution (see Table 2 in the Supporting Information).

The effects of an electric field, generated by a gate voltage, on the orbital energies of compound **9** in its triplet state was simulated through application of a dipolar homogeneous electric field. The calculations were performed at the UM06-2X/6-311+G(d,p) level using the triplet state geometry optimized at the same level in the absence of an applied electric field.

*Conflict of Interest:* The authors declare no competing financial interest.

*Acknowledgment.* B.O.J. acknowledges the Wenner-Gren foundation for a postdoctoral fellowship. M.G. gratefully acknowledges support by the National Science Foundation (CHE-1057930). J.F. and H.O. acknowledge financial support from the Swedish Research Council (2007-562 and 2008-3710). The Uppsala University UniMolecular Electronics Center (U<sup>3</sup>MEC) is acknowledged for fruitful discussions. The National Supercomputer Center

(NSC) in Linköping, Sweden, is acknowledged for generous allotment of computer time.

*Supporting Information Available:* Computational details, orbital energies of the separate monoradicals, relative electronic energies of the different states, molecular orbital schemes of compounds, Cartesian coordinates of the structures at (U)M06-2X/6-311+G(d,p), and complete reference 40. This material is available free of charge via the Internet at <http://pubs.acs.org>.

*Note Added after ASAP Publication:* After this paper was published on January 25, 2013 corrections were made for vector designations. The corrected version was reposted January 29, 2013.

## REFERENCES AND NOTES

- Wolf, S. A.; Awschalom, D. D.; Buhrman, R. A.; Daughton, J. M.; von Molnár, S.; Roukes, M. L.; Chtchelkanova, A. Y.; Treger, D. M. Spintronics: A Spin-Based Electronics Vision for the Future. *Science* **2001**, *294*, 1488–1495.
- Prinz, G. A. Magnetoelectronics. *Science* **1998**, *282*, 1660–1663.
- Otani, Y.; Kimura, T. Manipulation of Spin Currents in Metallic Systems. *Phil. Trans. R. Soc. A* **2011**, *369*, 3136–3149.
- Salikhov, R.; Abrudan, R.; Brussing, F.; Buschhorn, S.; Ewerlin, M.; Mishra, D.; Radu, F.; Garifullin, I. A.; Zabel, H. Precessional Dynamics and Damping in Co/Cu/Py Spin Valves. *Appl. Phys. Lett.* **2011**, *99*, 092509.
- Watson, S. K.; Potok, R. M.; Marcus, C. M.; Umansky, V. Experimental Realization of a Quantum Spin Pump. *Phys. Rev. Lett.* **2003**, *91*, 258301.
- Naber, W. J. M.; Faez, S.; van der Wiel, W. G. Organic Spintronics. *J. Phys. D: Appl. Phys.* **2007**, *40*, R205.
- Rocha, A. R.; García-suárez, V. M.; Bailey, S. W.; Lambert, C. J.; Ferrer, J.; Sanvito, S. Towards Molecular Spintronics. *Nat. Mater.* **2005**, *4*, 335–339.
- Bernot, K.; Pointillart, F.; Rosa, P.; Etienne, M.; Sessoli, R.; Gatteschi, D. Single Molecule Magnet Behaviour in Robust

Dysprosium-Biradical Complexes. *Chem. Commun.* **2010**, *46*, 6458–6460.

9. Fallah, F.; Esmailzadeh, M. Spin Transport Properties in an Organic Molecule in the Presence of Rashba Spin-Orbit Interaction. *Am. Inst. Phys. Adv.* **2011**, *1*, 032113.

10. Fransson, J.; Galperin, M. Spin Seebeck Coefficient of a Molecular Spin Pump. *Phys. Chem. Chem. Phys.* **2011**, *13*, 14350–14357.

11. Moreira, I. d. P. R.; Illas, F. A Unified View of the Theoretical Description of Magnetic Coupling in Molecular Chemistry and Solid State Physics. *Phys. Chem. Chem. Phys.* **2006**, *8*, 1645–1659.

12. Jacobs, S. J.; Shultz, D. A.; Jain, R.; Novak, J.; Dougherty, D. A. Evaluation of Potential Ferromagnetic Coupling Units: The bis(TMM) [bis(trimethylenemethane)] Approach to High-spin Organic Molecules. *J. Am. Chem. Soc.* **1993**, *115*, 1744–1753.

13. Rajca, A. Organic Diradicals and Polyradicals: From Spin Coupling to Magnetism? *Chem. Rev.* **1994**, *94*, 871–893.

14. Mas-Torrent, M.; Crivillers, N.; Rovira, C.; Veciana, J. Attaching Persistent Organic Free Radicals to Surfaces: How and Why. *Chem. Rev.* **2012**, *112*, 2506–2527.

15. Higashiguchi, K.; Yumoto, K.; Matsuda, K. Evaluation of the  $\beta$  Value of the Phenylene Unit by Probing Exchange Interaction between Two Nitroxides. *Org. Lett.* **2010**, *12*, 5284–5286.

16. Tomioka, H.; Iwamoto, E.; Itakura, H.; Hirai, K. Generation and Characterization of a Fairly Stable Triplet Carbene. *Nature* **2001**, *412*, 626–628.

17. Hase, S.; Shiomi, D.; Sato, K.; Takui, T. Phenol-Substituted Nitronyl Nitroxide Biradicals with a Triplet ( $S = 1$ ) Ground State. *J. Mater. Chem.* **2001**, *11*, 756–760.

18. Rajca, A.; Olankitwanit, A.; Rajca, S. Triplet Ground State Derivative of Aza-*m*-xylylene Diradical with Large Singlet-Triplet Energy Gap. *J. Am. Chem. Soc.* **2011**, *133*, 4750–4753.

19. Song, H.; Reed, M. A.; Lee, T. Single Molecule Electronic Devices. *Adv. Mater.* **2011**, *23*, 1583–1608.

20. Fransson, J.; Galperin, M. Inelastic Scattering and Heating in a Molecular Spin Pump. *Phys. Rev. B: Condens. Matter Mater. Phys.* **2010**, *81*, 075311.

21. Zhang, P.; Xue, Q.-K.; Xie, X. C. Spin Current through a Quantum Dot in the Presence of an Oscillating Magnetic Field. *Phys. Rev. Lett.* **2003**, *91*, 196602.

22. Fransson, J.; Zhu, J.-X. Vibrational Coherence in Electron Spin Resonance in Nanoscale Oscillators. *Phys. Rev. B* **2008**, *78*, 113307.

23. Zhao, Y.; Truhlar, D. The M06 Suite of Density Functionals for Main Group Thermochemistry, Thermochemical Kinetics, Noncovalent Interactions, Excited States, and Transition Elements: Two New Functionals and Systematic Testing of Four M06-class Functionals and 12 other Functionals. *Theor. Chem. Acc.* **2008**, *120*, 215–241.

24. McLean, A. D.; Chandler, G. S. Contracted Gaussian Basis Sets for Molecular Calculations. I. Second Row Atoms,  $Z = 11$ –18. *J. Chem. Phys.* **1980**, *72*, 5639–5648.

25. Krishnan, R.; Binkley, J. S.; Seeger, R.; Pople, J. A. Self-consistent Molecular Orbital Methods. XX. A Basis Set for Correlated Wave Functions. *J. Chem. Phys.* **1980**, *72*, 650–654.

26. Frisch, M. J.; Pople, J. A.; Binkley, J. S. Self-Consistent Molecular Orbital Methods 25. Supplementary Functions for Gaussian Basis Sets. *J. Chem. Phys.* **1984**, *80*, 3265–3269.

27. Becke, A. D. Density-Functional Thermochemistry. III. The Role of Exact Exchange. *J. Chem. Phys.* **1993**, *98*, 5648–5652.

28. Stephens, P. J.; Devlin, F. J.; Chabalowski, C. F.; Frisch, M. J. *Ab Initio* Calculation of Vibrational Absorption and Circular Dichroism Spectra Using Density Functional Force Fields. *J. Phys. Chem.* **1994**, *98*, 11623–11627.

29. Kinoshita, M. *p*-Nitrophenyl Nitronyl Nitroxide: The First Organic Ferromagnet. *Phil. Trans. R. Soc. A* **1999**, *357*, 2855–2872.

30. Barone, V.; Cacelli, I.; Ferretti, A. Magnetic Coupling in Bis-nitronylnitroxide Radicals: The Role of Aromatic Bridges. *J. Chem. Phys.* **2009**, *130*, 094306.

31. Neuhaus, P.; Grote, D.; Sander, W. Matrix Isolation, Spectroscopic Characterization, and Photoisomerization of *m*-Xylylene. *J. Am. Chem. Soc.* **2008**, *130*, 2993–3000.

32. Dowd, P. Trimethylenemethane. *Acc. Chem. Res.* **1972**, *5*, 242–248.

33. Wentholt, P. G.; Hu, J.; Squires, R. R.; Lineberger, W. C. Photoelectron Spectroscopy of the Trimethylenemethane Negative Ion. The Singlet-Triplet Splitting of Trimethylenemethane. *J. Am. Chem. Soc.* **1996**, *118*, 475–476.

34. Wentholt, P. G.; Kim, J. B.; Lineberger, W. C. Photoelectron Spectroscopy of *m*-Xylylene Anion. *J. Am. Chem. Soc.* **1997**, *119*, 1354–1359.

35. Borden, W. T.; Davidson, E. R. Effects of Electron Repulsion in Conjugated Hydrocarbon Diradicals. *J. Am. Chem. Soc.* **1977**, *99*, 4587–4594.

36. Limacher, P. A.; Lüthi, H. P. Cross-Conjugation. *WIREs Comput. Mol. Sci.* **2011**, *1*, 477–486.

37. Rajaraman, G.; Caneschi, A.; Gatteschi, D.; Totti, F. A DFT Exploration of the Organization of Thiols on Au(111): A Route to Self-Assembled Monolayer of Magnetic Molecules. *J. Mater. Chem.* **2010**, *20*, 10747–10754.

38. Dunning Jr., T. H.; Hay, P. J. In *Modern Theoretical Chemistry*; Schaefer, H. F., III, Ed.; Plenum: New York, 1976; Vol. 3; pp 1–28.

39. Hay, P. J.; Wadt, W. R. *Ab Initio* Effective Core Potentials for Molecular Calculations. Potentials for K to Au including the Outermost Core Orbitals. *J. Chem. Phys.* **1985**, *82*, 299–310.

40. Frisch, M. J.; Trucks, G. W.; Schlegel, H. B.; Scuseria, G. E.; Robb, M. A.; Cheeseman, J. R.; Scalmani, G.; Barone, V.; Mennucci, B.; et al., *Gaussian 09*, revision A.2; Gaussian Inc.: Wallingford CT, 2009.